Title

The role of FUT8-catalyzed core fucosylation in Alzheimer's amyloid-β oligomer-induced activation of human microglia

Authors

Jin, Lee-Way
di Lucente, Jacopo
Mendiola, Ulises Ruiz
et al.

Peer reviewed

The role of FUT8-catalyzed core fucosylation in Alzheimer's amyloid-β oligomer-induced activation of human microglia

Lee-Way Jin[1], **Jacopo di Lucente**[1], **Ulises R. Mendiola**[1], **Xinyu Tang**[2], **Angela M. Zivkovic**[2], **Carlito B. Lebrilla**[3], **Izumi Maezawa**[1]

[1]Department of Pathology and Laboratory Medicine and M.I.N.D. Institute, University of California Davis Medical Center, 2805 50th Street, Sacramento, CA 95817

[2]Department of Nutrition, University of California, Davis, CA 95618

[3]Department of Chemistry, University of California, Davis, CA 95618

Abstract

Fucosylation, especially core fucosylation of N-glycans catalyzed by α1-6 fucosyltransferase (fucosyltransferase 8 or FUT8), plays an important role in regulating the peripheral immune system and inflammation. However, its role in microglial activation is poorly understood. Here we used human induced pluripotent stem cells-derived microglia (hiMG) as a model to study the role of FUT8-catalyzed core fucosylation in amyloid-β oligomer (AβO)-induced microglial activation, in view of its significant relevance to the pathogenesis of Alzheimer's disease (AD). HiMG responded to AβO and lipopolysaccharides (LPS) with a pattern of pro-inflammatory activation as well as enhanced core fucosylation and FUT8 expression within 24 hours. Furthermore, we found increased FUT8 expression in both human AD brains and microglia isolated from 5xFAD mice, a model of AD-like cerebral amyloidosis. Inhibition of fucosylation in AβO-stimulated hiMG reduced the induction of pro-inflammatory cytokines, suppressed the activation of p38MAPK, and rectified phagocytic deficits. Specific inhibition of FUT8 by siRNA-mediated knockdown also reduced AβO-induced pro-inflammatory cytokines. We further showed that p53 binds to the two consensus binding sites in the *Fut8* promoter, and that p53 knockdown abolished FUT8 overexpression in AβO-activated hiMG. Taken together, our evidence supports that FUT8-catalyzed core fucosylation is a signaling pathway required for AβO-induced microglia activation and that FUT8 is a component of the p53 signaling cascade regulating microglial behavior. Because microglia are a key driver of AD pathogenesis, our results suggest that microglial FUT8 could be an anti-inflammatory therapeutic target for AD.

Graphical Abstract

Address Correspondence to: Izumi Maezawa, Ph.D., Department of Pathology and Laboratory Medicine, University of California Davis Medical Center, Sacramento, CA 95817, USA, Fax: (916) 703-0370; imaezawa@ucdavis.edu.
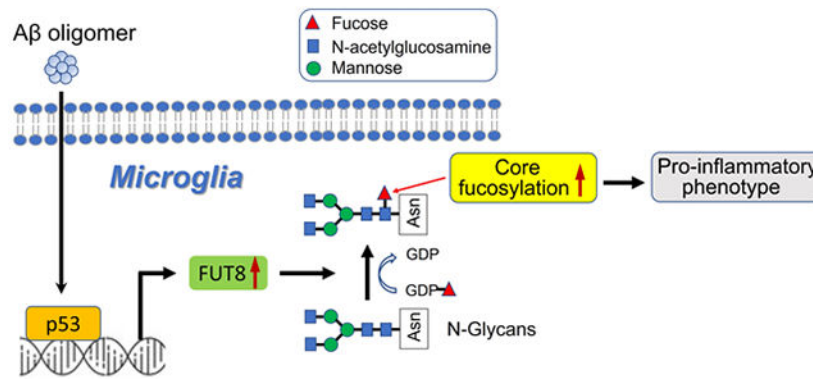
Keywords

Microglia; Alzheimer's; fucosylation; glycosylation; amyloid; fucosyltransferase; p53

INTRODUCTION

Microglia represent the immune system of the mammalian brain and constantly survey their microenvironment to maintain brain homeostasis (Nimmerjahn, Kirchhoff, & Helmchen, 2005). By orchestrating neuroinflammation, microglia play a pivotal role in the initiation and progression of Alzheimer's disease (AD), the most common cause of dementia in elderly populations. A generally accepted hypothesis states that activated microglia release cytotoxic substances and pro-inflammatory cytokines that cause neuronal damage and aggravate Alzheimer's disease pathology (Heneka et al., 2015). While multiple factors may cause microglial activation in AD, early studies have established that different species of Aβ aggregates are potent stimulants of microglia. Among them, we and others found that the small soluble Aβ oligomer (AβO) assembled from Aβ42 peptide provides far stronger stimulation to induce microglial activation (Maezawa et al., 2017; Maezawa, Zimin, Wulff, & Jin, 2011). Aβ aggregates are recognized by a range of microglial pattern recognition receptors to induce mainly pro-inflammatory responses that could mediate Aβ-induced neurotoxicity, impair phagocytic function, and prime microglia to enhance their sensitivity and reactivity to inflammatory stimuli (Leng & Edison, 2021). Understanding mechanisms of such activations could provide microglial targets for interventions to halt AD progression.

In the brain, over 70% of proteins and a large fraction of the lipids are glycosylated (Tena & Lebrilla, 2021). These common structure modifications are considered to mediate cell-cell communication via interacting with glycan-binding proteins or other signaling processes. Among brain glycans, sialylated and fucosylated ones are most abundant and dynamically regulated during brain development and maturation, suggesting their functional significance (Gaunitz, Tjernberg, & Schedin-Weiss, 2021; Lee et al., 2020). Sialic acid is the most abundant component in glycoconjugates and is well studied in the brain (Schnaar, Gerardy-Schahn, & Hildebrandt, 2014). It regulates microglia function and neuron-microglia interactions in part via being the ligand for siglecs, including siglec-3 (CD33) which is a risk factor for late-onset AD (Estus et al., 2019; Puigdellivol, Allendorf, & Brown, 2020). After sialic acid, L-fucose is the 2nd most abundant but much less studied. Accumulating evidence

from peripheral tissues indicates significant roles of protein fucosylation in development, leukocyte adhesion, gut microbiome maintenance, cancer metastasis, and many other physiological and pathological processes (Schneider, Al-Shareffi, & Haltiwanger, 2017). A small number of studies have shown that fucosylation affects processes involved in learning and memory, such as long-term potentiation, neurite outgrowth and migration, synapse formation, among others (Murrey et al., 2006; Schneider et al., 2017). However, how fucosylation affects microglial function or dysfunction in brain diseases is poorly understood, despite its known roles in peripheral immune regulation (Schneider et al., 2017).

In this study, we investigated the role of fucosylation, particularly FUT8-dependent core fucosylation, in AβO-induced activation of human microglia. In N-glycans, L-fucose is predominantly incorporated into oligosaccharides via α−1,6-linked to the innermost core N-acetylglucosamine residue as core fucose (Skurska et al., 2022). In mammals, FUT8 is the only α−1,6-fucosyltransferase that is uniquely responsible for core fucosylation (Ihara et al., 2007; Kotzler, Blank, Bantleon, Spillner, & Meyer, 2012; Yang & Wang, 2016). Our rationale is that core fucosylation of N-glycans plays important roles in regulating the peripheral immune system and inflammation (Kizuka et al., 2017; Ng et al., 2018) but its role in microglia-orchestrated neuroinflammation has been little studied. In addition, our meta-analysis of published large-scale transcriptomics data of AD brain samples from the Mount Sinai cohort (M. Wang et al., 2018) revealed a significant increase of *Fut8* transcript in the AD parahippocampal gyrus. To better model human microglial pathology, we employed human induced pluripotent stem cell (iPSC)-derived microglia (hiMG) as a major model rather than the widely used primary cultures from neonatal rodents, based on the insight that rodents are generally a better model for neuronal pathology than they are for microglial pathology (Penney, Ralvenius, & Tsai, 2019), and that for optimal translational validity, human microglia are recommended to be used to identify human-relevant molecular pathways and therapeutic targets (Smith & Dragunow, 2014).

METHODS

Human iPSC culture and microglia differentiation

Human iPSCs were obtained from ALSTEM.INC. (Richmond, CA). The line used in this study was Human iPS Cell Line 26 (Episomal, CD34+, ApoE3). Cells were plated onto Matrigel (Fisher) coated plates and cultured with mTeSR plus (Stemcell Technology). For microglia differentiation, we followed the a previously published protocol (Haenseler et al., 2017). Briefly, 2×10^6 iPSCs were plated onto Aggrewell 800 plates (Stemcell Technology) to form embryoid bodies (EBs) in mTeSR1 supplemented with Bone Morphogenetic Protein 4 (BMP4, 50 ng/ml)/Vascular Endothelial Cell Growth Factor (VEGF, 50 ng/ml)/ Stem Cell Factor (SCF, 20 ng/ml) and culture for four days with daily medium change. On the fifth day, EBs were plated onto gelatin coated 6-well plates with 20 EBs per well in X-VIVO15 (Lonza) supplemented with M-CSF (100ng/ml), IL-3 (25ng/ml), Glutamax (2mM), Penicillin/streptomycin (100U/ml and 100ug/ml) and β-mercaptoethanol (55uM), and the medium was changed weekly. After 3-4 weeks, floating primitive macrophage precursor (PMP) were collected and plated onto 12-well plates (5×10^4 cells/well), 6-well plates (3×10^5 cells/well), or 100 mm dishes (1.5×10^6 cells) and differentiated in microglia

differentiation medium (Advanced DMEM/F12 supplemented with IL-34 (100ng/ml), GM-CSF (10ng/ml), N2 supplement (1x), Glutamax (2mM), Penicillin/streptomycin (100U/ml and 100ug/ml) and β-mercaptoethanol (55uM)) for two weeks.

Aβ oligomer (AβO) preparation and treatment

AβO composed of Aβ1-42 peptide was prepared following a standard procedure (Lambert et al., 1998) with a modification that the HFIP treated Aβ1-42 peptide (Bachem) was dissolved in DMSO and then diluted with Advanced DMEM/F12 culture medium instead of the F12 medium originally described, followed by incubation at 4°C for 24 h and 10 min centrifugation at 10,000 x rpm at 4°C. This preparation of AβO has been extensively characterized in our laboratory (Maezawa et al., 2011). Briefly, to ensure consistency of quality, a random sample from each batch was chosen and imaged using electron microscopy and atomic force microscopy to characterize the size and shape of the aggregates. The biological activities of each batch were confirmed by determining for AβO the neurotoxic activity, synaptic binding activity, and ability to rapidly induce exocytosis of MTT formazan, as described previously (Maezawa et al., 2011, Hong et al., 2007). For all microglial activation experiments, AβO was administered at 3 μM in the medium. For the application of fucosylation inhibitors, microglia were pre-incubated with 250 μM 2-Fluorofucose (SynChem Inc) or 50 μM 6-Alkynyl-Fucose (Fisher) for 1 hr before the addition of AβO.

SiRNA-mediated gene knockdown

To knockdown *Fut8* and *p53*, cells were transfected with small interference RNAs (siRNAs) using HiPerFect transfection reagent (Qiagen) according to the manufacturer's instructions. SiRNA to human *Fut8* and *p53* sequences were purchased from Qiagen (*Fut8*:GS2530 and *p53*:GS7157). As a transfection control, All Stars Negative Control siRNA (Qiagen) was used. Gene knockdown was confirmed by qPCR. For AβO activation after gene knockdown, at 24 hrs after transfection, AβO was added without changing the medium and cells were further cultured for 24 hrs.

qPCR

Total RNA from cultured cells and brain tissues were extracted using RNeasy Plus Mini Kit and RNeasy Plus Universal Mini kit (Qiagen), respectively. cDNA was synthesized using 100 ng RNA and iScript Reverse Transcription Supermix (BioRad). Quantitative real-time polymerase chain reaction (qPCR) was performed using SsoFast™ EvaGreen Supermix and CFX96 qPCR system (BioRad). The forward/reverse primer sequences used are listed in Table 1. Gene expression was normalized to an endogenous gene, β-actin. Relative cDNA levels for the target genes were analyzed by the $2^{-\Delta\Delta Ct}$ method.

Microglia isolation from mouse brains

Microglia were acutely isolated from adult mouse brains as described (Jin et al., 2019). Briefly, brains were dissociated enzymatically with a Neural Tissue Dissociation Kit (Miltenyi Biotec). Microglia were subsequently purified by the magnetic-activated cell sorting (MACS) using anti-CD11b magnetic beads (Miltenyi Biotec). Total RNA from

acutely isolated microglia was extracted using RNeasy Plus Mini Kit (Qiagen), reverse-transcribed and pre-amplified with Ovation PicoSL WTA System V2 kit (NuGen, San Carlos, CA) and analyzed by qPCR.

Fluorescent detection of fucosylation

After AβO treatment, cells were fixed with 4% paraformaldehyde in PBS (10 mM NaH2PO4, 150 mM NaCl, pH7.4). For flow cytometry analysis, cells were incubated with PBS with 0.1% Tween20 (PBS-T) for 30 min and then incubated with AAL-FL (1:300, Vector Lab) or LCA-FL (1:300, Vector Lab) for 30min at room temperature. After washing with PBS, cells were gentry scraped in PBS and analyzed by flow cytometry using a BD Accuri™ C6 Plus flow cytometer (BD Biosciences). For visualization of lectin staining, fixed cells were incubated with PBS-T (for LCA) or 3% BSA in PBS-T (for PhoSL) for 1 hr and then incubated with LCA-FL (1:1000) in PBS or Afuc PhoSL-mIgG2c (1:1000, Antagen Biosciences) in 1%BSA in PBS overnight at 4°C. (Afuc PhoSL-mIgG2c is a fusion protein of PhoSL with mIgG2c Fc devoid of any fucose in its glycan which has been shown to have considerably enhanced binding specificity to core fucosylation.) For PhoSL staining, cells were further incubated with anti-mouse Alexa488 conjugated secondary antibody (1:1,000, Invitrogen) for 1 hr. After washing, cells were incubated with Hoechst33342 (5 μg/ml) for 20 min. Fluorescence images were taken by ImageXpress Pico (Molecular Devices). Fluorescence intensity and cell number were quantified by ImageJ program.

ELISA quantification

ELISA quantification of cytokines were conducted as previously described (Maezawa et al., 2011). Briefly, conditioned medium was collected and centrifuged at 10k x rpm, 5min to remove cell debris. Supernatants were stored at −20° until use. Concentrations of IL-1ß and TNF-α were measured using the Quantikine sandwich ELISA kit (R&D systems, Minneapolis, MN).

Western blot and lectin blot

Cells were lysed in cell lysis buffer (140 mM NaCl, 10 mM Tris-HCl, pH 8.0, 1 mM EDTA, 0.5 mM EGTA, 1% Tx100, 0.1% SDS, 0.1% Sodium Deoxycholate) with protease inhibitor cocktail and phosphatase inhibitor (Sigma). Equivalent amounts of protein (15 μg for western blot and 5 μg for lectin blot) were analyzed by 4–20% Tris-Glycin gel electrophoresis (Invitrogen). Proteins were transferred to PVDF membranes and probed with antibodies or lectins. Visualization was enabled using enhanced chemiluminescence (GE Healthcare Pharmacia). The following primary antibodies and lectins (dilutions) were used: anti-Fut8 (1:1000, Abcam), anti-p53 (1:1000, Cell Signaling), anti-phosphor-p38MAPK (1:1000, Cell Signaling), anti-p38MAPK (1:1000, Cell Signaling), anti-β-actin (1:2000, Cell Signaling), AAL-HRP conjugated (1:10,000, Vector Lab), LCA-biotinylated (1:10,000, Vector Lab), and PhoSL (1:10,000, Antagen Biosciences). Secondary antibodies for western blotting were HRP-conjugated anti-rabbit or anti-mouse antibodies (1:1000, Cell Signaling). Secondary reagents for lectin blotting were HRP conjugated Streptavidin (1:10,000, Vector Lab) and anti-mouse antibody (1:10,000, Cell Signaling).

Chromatin immunoprecipitation (ChIP)

Cells (2 x 10^6 cells/100 mm dish) were treated with AβO (3 μM) for 24 hrs and the ChIP assay was performed using Pierce Agarose ChIP Kit (Fisher Scientific) combined with a ChIP validated antibody called ChIPAb+ p53 (Millipore Sigma) according to the manufacture's instruction. PCR was performed using Platinum™ Hot Start PCR Master Mix (Fisher) and analyzed by electrophoresis in 1.5% agarose gel. Primers for specific p53 binding sites in human *FUT8* promotor were synthesized according to the published sequences (Okagawa et al., 2016).

Phagocytosis assay

HiMG (7 x 10^4/well in 12-well plates) were treated with AβO (3 μM) with and without 2FF. Twenty-four hrs later, cells were incubated with pHrodo Green BioParticles (5 μg/ml, Invitrogen) or Aβ1-42 monomer-FITC conjugated (500 nM, Bachem) for 1hr. Cells were then washed three times, 5 min each, with PBS. For cells being tested for phagocytosis of Aβ1-42 monomer-FITC conjugated, they were further incubated with 0.4% Trypan blue for 1min to quench surface-bound Aβ. The cells were then analyzed by flow cytometry and/or cell imaging. For flow cytometry, cells were gently scraped with 1% BSA in PBS and analyzed by a BD Accuri C6 plus flow cytometer (BD Biosciences). For cell imaging, cells were fixed with 4% paraformaldehyde for 20 min, and fluorescence or phase contrast images were taken by a ImageXpress Pico scanner (Molecular Devices) or a fluorescence microscope (Nikon).

In some experiments, cells were further stained with Iba1 antibody (1:700, Biocare Medical) followed by anti-rabbit Alexa594 conjugated (1:1000, Invitrogen). Fluorescence intensity was quantified by ImageJ and bright images were used for counting the number of cells.

Mice.—Tg6799 5xFAD [B6SJL-Tg(APPSxFILon,PSEN1*M146L*L286V)6799Vas/ Mmjax] mice on the C57Bl/6 background were originally obtained from Dr. Robert Vassar, Ph.D., Northwestern University. Roughly equal numbers of male and female mice were used. All protocols involving mouse models were approved by the Institutional Animal Care and Use Committee.

Human brain samples

All tissues were collected and provided by the University of California Davis Alzheimer's Disease Research Center (P30 AG072972). Written informed consent, including consent for autopsy, was obtained from study participants or, for those with substantial cognitive impairment, a caregiver, legal guardian or other proxy. Study protocols were reviewed and approved by the Institutional Review Board (IRB). For postmortem diagTwlnosis, we followed the National Institute on Aging-Alzheimer's Association guideline for the neuropathologic assessment of AD. The brain tissues used for the current study were snap frozen during autopsy and was stored in −80°C before use. RNA samples from the middle temporal cortex of 12 AD (7 males and 5 females) and 12 control cognitively normal subjects (6 males and 6 females) were used. The average age of the AD group was 78.8 ± 3.4 years and that of the control group 84.3 ± 2.5 years. All AD subjects had a

neurofibrillary pathology stage of 6 and the control subjects had a neurofibrillary pathology stage of 2 (Alafuzoff et al., 2008).

Statistical analysis

Statistical analysis was performed using GraphPad Prism 9 software. All data are presented as means ± s.e.m. Comparison of the mean values was performed using unpaired Student's two-tailed t-test, on-way ANOVA, or two-way ANOVA with Tukey's *post hoc* test. Exact sample sizes and statistical test used for each comparison were provided in corresponding figure legends. $P < 0.05$ was considered to be statistically significant.

RESULTS

Activation of human iPSC-derived microglia by AβO is associated with enhanced core fucosylation

To study AD-related mechanisms in human microglia, we followed a standard protocol (Haenseler et al., 2017) to differentiate a human iPS cell line into microglia-like cells (Fig. 1). To confirm the differentiation, gene expression of mature microglia markers, *C1q, P2ry12, Tmem119,* and *Trem2*, was analyzed by qPCR. The levels of all these markers were significantly increased compared to original iPS cells, with the exception of *Tmem119*, which were also increased compared to primitive macrophage precursor (PMP) cells. Immunostaining showed the reactivities to PU.1, a major regulator of microglial gene expression (Rustenhoven et al., 2016), and Iba1, a well-established microglial marker, further supporting microglial differentiation. To assess their functional responses to inflammatory stimuli, microglia were treated with LPS or AβO and the expressions of pro-inflammatory cytokines were analyzed. In a dose-response study (Supplementary Fig. 1), we found that HiMG responded to AβO in a dose-dependent manner and chose AβO containing 3 μM Aβ1-42 peptide (designated as 3 μM AβO) as the optimal concentration for subsequent experiments. Both LPS (100 ng/ml) and AβO (3 μM) significantly increased the expression of pro-inflammatory cytokines IL-1β, TNF-α and IL-6. Phase contrast images showed activated microglia morphology with reduced ramifications and transition to ameboid morphology (Fig. 1).

To assess if hiMG activation is accompanied by enhanced fucosylation of glycoconjugates, we conducted flow cytometry studies using the lectin Aleuria Auratia Lectin (AAL) which recognizes α−1,6 core fucosylation and also α−1,2 and α−1,3 terminal fucosylation (Olausson, Tibell, Jonsson, & Pahlsson, 2008; Romano et al., 2011). Both LPS and AβO treatments increased fucosylation to comparable degrees (Fig. 2A). Using AβO-stimulated hiMG as an example, the enhanced AAL-binding was further illustrated by fluorescence microscopy (Fig. 2B) and lectin blot (Fig. 2C).

Due to our interest in AD, we subsequently focused on AβO-treated iMG. Also we further used two lectins specific to core fucosylation, the predominant form of L-fucose modifications in glycoconjugates. Lens culinaris agglutinin (LCA) recognizes only bi-antennary N-glycans with a core fucose (Tateno, Nakamura-Tsuruta, & Hirabayashi, 2009), and *P. squarrosa* lectin (PhoSL) was reported to recognize core fucose even more specific

than LCA (Kobayashi et al., 2012). The two lectins recognized different and overlapping sets of fucosylated glycoconjugates in lectin blots, and the reactivities of both were enhanced in AβO-treated microglia (Fig. 2D). The increase in core fucosylation was further confirmed by quantification of fluorescence intensity under microscopy (Fig. 2E)

FUT8 expression is upregulated in AβO-stimulated hiMG and in human AD and 5xFAD mouse brains

FUT8 is the only α−1,6-fucosyltransferase expressed in mammals that is uniquely responsible for the core fucosylation of N-glycoproteins (Ihara et al., 2007; Kotzler et al., 2012; Yang & Wang, 2016). Interestingly, our meta-analysis of the large-scale transcriptomic data deposited by the Mount Sinai Brain Bank (MSBB) study (M. Wang et al., 2018) showed that *Fut8* is one of the most abundant fucosyltransferase transcripts in the human brain and is upregulated in the parahippocampal gyrus ($p = 0.041$). We confirmed this change by qPCR on an independent set of middle temporal cortex samples obtained from the University of California Davis Alzheimer's Disease Research Center and found a ~1.8 fold upregulation of *Fut8* transcript in AD subjects compared to age-matched cognitively normal control subjects (Fig. 3A). We therefore asked whether AβO-induced core fucosylation in HiMG was related to increased FUT8 protein level. Western blotting showed a ~1.5 fold increase in FUT8 protein level in AβO-treated iMG (Fig. 3B). To evaluate if this upregulation is also observed *ex vivo*, we isolated microglia from the forebrain of 5xFAD mice, which harbor five familial mutations of APP and PSEN1 genes and show robust Aβ production and Aβ-associated neuroinflammation (Oakley et al., 2006). Soluble AβO made of Aβ42 is a major species of *Aβ* aggregates in 5xFAD mice (Hong et al., 2010), which can stimulates microglia (Jin et al., 2019). Due to the limited quantity of microglial material isolated from each mouse, we were only able to conduct qPCR evaluation of the transcript level, which showed a ~2.8 fold increase in *Fut8* in 5xFAD microglia (Fig. 3C). By comparison, total forebrain transcript levels of FUT8 were not different between 5xFAD and WT mice, although the protein levels showed a ~1.5 fold increase in 5xFAD mice (Fig. 3D). These results suggest an amyloid Aβ-related increase in FUT8 expression in AD brain tissue, and this increase is accentuated in microglia.

Inhibition of fucosylation dampens AβO-induced hiMG activation and normalizes phagocytotic capacity

To determine the role of fucosylation, in particular core fucosylation, in AβO-induced iMG activation, we used a widely used fucosylation inhibitor called 2-fluoro-fucose (2FF) and in some experiments also used 6-alkynyl-fucose (6AF). 2FF is a peracetylated derivative of L-fucose that can be converted to its corresponding nucleotide sugars, guanosine diphosphate (GDP)-2-deoxy-2-fluoro-L-Fucose, thus competing with and suppressing GDP-L-fucose, the natural substrate of fucosyltransferases. 2FF particularly suppresses core fucosylation (Rillahan et al., 2012). 6AF is a specific and potent inhibitor of GDP-4-keto-6-deoxymannose 3,5-epimerase (FX) (Kizuka et al., 2017) that catalyzes the last step of the *de novo* pathway for GDP-fucose production. Their effects on hiMG core fucosylation were confirmed as the reactivities of LCA and PhoSL in AβO-treated iMG were reduced in cells co-treated with 2FF or 6AF (Fig. 2D and 2E). Flow cytometry studies further confirmed that 2FF reduced AAL and LCA reactivities in AβO-treated hiMG (Fig. 4A). As expected,

2FF and 6AF had no impact on the FUT8 protein level (Fig. 4B), indicating that their effects were not mediated by FUT8 downregulation. As a negative control, 2,4,7,8,9-Penta-O-acetyl-N-acetyl-3-fluoro-b-D-neuraminic acid methyl ester (3FS), a sialylation inhibitor (Zhou, Xie, Lam, & Lebrilla, 2021), did not reduce fucosylation (Fig. 4A).

We examined whether fucosylation is required for several aspects of AβO-induced hiMG activation. AβO-stimulated increased expression of pro-inflammatory cytokines IL-1β and TNF-α was significantly reduced by 2FF and 6AF co-treatment, at both transcript (Fig. 4C) and protein levels (Fig. 4D). One of signaling events involved in microglial activation is sustained p38MAPK phosphorylation (Bachstetter et al., 2011). We found that the sustenance of p38MAPK phosphorylation was abolished when AβO-stimulated hiMG were co-treated with 2FF, despite the presence of an initial response at 10 min (Fig. 4E). The other major function of microglia is phagocytosis. We found that AβO impaired this function of hiMG, tested by their ability to phagocytose fluorescent BioParticles (Kapellos et al., 2016). Co-treatment with 2FF rectified this deficit, as quantified by flow cytometry (Fig. 5A) or fluorescent microimaging using an automated scanner (Fig. 5B and 5C). We also tested the ability of hiMG to phagocytose FITC-labeled Aβ monomer and showed a similar result (Fig. 5D and 5E)

As fucosylation inhibitors inhibit core fucosylation as well as other fucosylations on glycan antennae, such as α1-3 or α1-4 linkage to N-acetylglucosamine or α1-2 linkage to galactose, we employed siRNA-mediated *Fut8* gene knockdown to more specifically examine the role of FUT8-catalyzed core fucosylation. We tested four FUT8 siRNAs and selected two most effective ones, #5 and #8, which induces *Fut8* knockdown to 50% and 17% of the control siRNA level, respectively (Fig. 6A). Both siRNAs substantially reduced the transcripts of IL-1β, IL-6, and TNFα to levels comparable to the non-AβO control group (Fig. 6B). The lack of differential cytokine reduction by two siRNAs with different *Fut8* knockdown potencies suggest that partial inhibition of core fucosylation may be sufficient for full-scale inhibition of AβO-induced cytokine responses.

P53 drives FUT8 overexpression in AβO-activated hiMG

FUT8 was identified as a direct transcriptional target of p53 in hepatocellular carcinoma cells (Okagawa et al., 2016). However, such a mechanism has not been established in other cell types. Because p53 influences microglial behavior via supporting the adoption of a proinflammatory phenotype (Jayadev et al., 2011), we asked whether FUT8 upregulation in AβO-activated hiMG is mediated by p53. Immunoblotting showed a ~1.65 fold increase in p53 protein level following AβO treatment, indicating an association with FUT8 upregulation (Fig. 3B, 4B). Two siRNAs were used to induce *p53* knockdown to 40% and 45% of the control level, respectively (Fig. 7A). The expected impact of *p53* knockdown on microglial pro-inflammatory responses was confirmed by the suppression AβO-induced TNF-α and IL-1β expression (Fig. 7B). Both siRNAs also abolished AβO-induced FUT8 over-expression (Fig. 7C), indicating that FUT8 overexpression is downstream of p53. To test if p53 directly interacts with *Fut8* gene promoter in hiMG, we conducted chromatin immunoprecipitation (ChIP) assays to evaluate whether p53 binds to the two conserved p53 binding DNA sequences (BS1 and BS2) within 2 kb upstream of the human FUT8 promoter

(Okagawa et al., 2016). AβO-treated iMG showed enhanced binding of p53 to both BS1 and BS2 while control-treated iMG showed minimal binding (Fig. 7D). This pattern is similar to that of p53 binding to a promoter sequence of p21/waf1, encoding a cyclin-dependent kinase inhibitor protein which is an established downstream effector of p53 (Kumari & Jat, 2021; Saramaki, Banwell, Campbell, & Carlberg, 2006). Taken together, the results suggest that FUT8-mediated core fucosylation is downstream to and instrumental in the p53-orchestrated mechanisms to support AβO-induced proinflammatory phenotype of microglia (Aloi, Su, & Garden, 2015).

DISCUSSION

There is a dearth of knowledge about the role of protein fucosylation in microglial activation, despite its known significant roles in immune regulation and inflammation in peripheral systems. Furthermore, available data regarding the activation signaling pathways using human microglia models are quite limited as a large majority of prior studies were conducted using rodent microglia. We therefore investigated core fucosylation in AβO-activated human iPSC-derived microglia and found that such an activation is associated with increased α1, 6 core fucosylation, as well as upregulations of FUT8 and p53. Our evidence supports a mechanism in which p53 upregulates FUT8 and subsequently, as expected, FUT8 is responsible for increased core fucosylation. Furthermore, we showed that FUT8-catalyzed core fucosylation is required for AβO-induced hiMG activation. Because microglia-orchestrated neuroinflammation is a key driver of AD pathogenesis, our results suggest that microglial FUT8 could be an anti-inflammatory therapeutic target for AD.

The only article we are aware of investigating the role of FUT8 in microglia activation is by Lu et al., who reported that *Fut8*-knockout mouse BV2 microglia cell line showed enhanced pro-inflammatory response following LPS stimulation, and concluded that core fucosylation negatively regulates the states of neuroinflammation by modulating the sensitivity of microglia to inflammatory mediators (Lu et al., 2019). Apparently, this notion cannot be generalized to human microglia stimulated by AβO, as we found that *Fut8* knockdown diminished the pro-inflammatory response to AβO. While this discrepancy may reflect interspecies and model differences, we consider that BV2 is not an optimal model to study FUT8-mediated microglia responses. This is because, in addition to the well-known limitations of BV2 (Stansley, Post, & Hensley, 2012), FUT8 is a critical component of growth and progression of multiple cancers (Bastian, Scott, Elliott, & Munkley, 2021), making it difficult to use a rapidly growing tumor-like cell line such as BV2 to parse out impacts of FUT8 on proinflammatory response *per se*. This is particularly so when no pro-inflammatory cytokine data were reported as a part of confirmatory evaluation by Lu et al (Lu et al., 2019). In this regard, we consider that human iPSC-derived microglia would provide a model with stronger validity and human relevance. Lu et al. also reported increases in basal and LPS-stimulated microglia count in *Fut8*–/– mouse brain. While interesting, these increases may reflect broader complex brain and systemic pathological environments and do not directly reflect the microglial inherent FUT8-regulated properties relevant to pro-inflammatory responses. *Fut8*–/– mice manifest early death during postnatal development (30% surviving 3 days after birth and few surviving over 1 month), with survivors showing severe growth retardation and emphysema-like changes in the lung

(Wang et al., 2006). Behavioral phenotyping of 2.5-3.5 months old *Fut8–/–* mice on a different genetic background to support slightly better survival showed multiple behavioral abnormalities consistent with a schizophrenia-like phenotype (Fukuda et al., 2011). While these studies support a critical role of FUT8 in lung and brain development, future studies using microglia-targeted conditional knockout approaches would be needed to parse out how FUT8 affects the inherent immunometabolic properties of microglia and microglia-orchestrated neuroinflammation in the mature brain.

Our results provide rationales to further investigate specific FUT8-downstream molecular pathways via which core fucosylation regulates microglial activation. Based on available data from non-microglia cells, core fucosylation may affect a few key signaling molecules involved in microglia activation. A possible pathway involves core fucosylation of the receptor for transforming growth factor-β (TGF-β), which is a key regulator of microglial maturation, homeostasis and activation (Spittau, Dokalis, & Prinz, 2020). *Fut8–/–* mice showed substantially dysregulated TGF-β signaling in the lung and fibroblasts, manifested by disrupted extracellular matrix homeostasis and a significantly high level of matrix metalloproteinase expression (X. Wang et al., 2005). In contrast, FUT8 overexpression to increase core fucosylation of TGF-β receptor complexes enhanced TGF-β signaling in breast cancer cells, promoting cancer invasion and metastasis (Tu, Wu, Lin, Kannagi, & Yang, 2017). Other possible mechanisms include the role of core fucosylation in α3β1 Integrin function (Zhao et al., 2006) or epidermal growth factor receptor (EGFR) signaling (X. Wang et al., 2006), both of which may affect microglial migration and activation. Thus, core fucosylation in microglia may regulate multiple signaling pathways that regulate key aspects of microglial function, including their interactions with other neural cells and their migration.

P53 has been identified as a master transcriptional regulator of microglial behavior (Aloi et al., 2015; Sullivan, Galbraith, Andrysik, & Espinosa, 2018). Mouse studies showed that p53 activity supports the adoption of a proinflammatory phenotype, while p53 deficiency promotes phagocytosis and gene expression associated with alternative activation and anti-inflammatory functions (Jayadev et al., 2011). Multiple lines of evidence have associated p53 upregulation/activity, including that in microglia, with the pathogenesis of AD (Hooper et al., 2007; Kitamura et al., 1997; Li, Zi, Hou, & Tu, 2017; Tan, Wang, Song, & Jia, 2012). Our data is consistent with all above notions. We further identified that FUT8 is a novel target gene for p53 in human microglia. AβO-induced FUT8 expression is dependent on p53 activity, and, following AβO stimulation, p53 directly binds to two FUT8 gene promoter sites identified by their high homology to p53-DNA consensus binding sequence. Also consistent with the p53-activated proinflammatory activation pattern is the observation that phagcytotic activity was suppressed by AβO, which would compromise the microglia-mediated clearance mechanisms critical for brain homeostasis. We found that this negative regulation could be rectified by inhibition of core fucosylation, suggesting a role of FUT8 in mediating p53-orchestrated regulation of phagocytosis. Taken together, our data reveal a new insight that FUT8-catalyzed core fucosylation is a key component of the p53 signaling network in microglia.

While this study has focused on microglia which indeed show accentuated upregulation of FUT8, it is noteworthy that FUT8 expression is upregulated in human AD and 5xFAD brains, not limited to microglia. Therefore, FUT8 and its resulting core fucosylation may play a broader role in AD pathogenesis in addition to microglia activation. Our data warrant further comprehensive studies of the roles of abnormal core fucosylation in AD to include neurons, astrocytes, and neuron-glia interaction.

Supplementary Material

Refer to Web version on PubMed Central for supplementary material.

Acknowledgement:

Data Sharing:

The data that support the findings of this study are available from the corresponding author upon reasonable request.

References

Alafuzoff I, Arzberger T, Al-Sarraj S, Bodi I, Bogdanovic N, Braak H, … Kretzschmar H (2008). Staging of neurofibrillary pathology in Alzheimer's disease: a study of the BrainNet Europe Consortium. Brain Pathol, 18(4), 484–496. doi:10.1111/j.1750-3639.2008.00147.x [PubMed: 18371174]

Aloi MS, Su W, & Garden GA (2015). The p53 Transcriptional Network Influences Microglia Behavior and Neuroinflammation. Crit Rev Immunol, 35(5), 401–415. doi:10.1615/critrevimmunol.v35.i5.40 [PubMed: 26853851]

Bachstetter AD, Xing B, de Almeida L, Dimayuga ER, Watterson DM, & Van Eldik LJ (2011). Microglial p38alpha MAPK is a key regulator of proinflammatory cytokine up-regulation induced by toll-like receptor (TLR) ligands or beta-amyloid (Abeta). J Neuroinflammation, 8, 79. doi:10.1186/1742-2094-8-79 [PubMed: 21733175]

Bastian K, Scott E, Elliott DJ, & Munkley J (2021). FUT8 Alpha-(1,6)-Fucosyltransferase in Cancer. International Journal of Molecular Sciences, 22(1). doi:ARTN 455 10.3390/ijms22010455 [PubMed: 33466384]

Estus S, Shaw BC, Devanney N, Katsumata Y, Press EE, & Fardo DW (2019). Evaluation of CD33 as a genetic risk factor for Alzheimer's disease. Acta Neuropathol, 138(2), 187–199. doi:10.1007/s00401-019-02000-4 [PubMed: 30949760]

Fukuda T, Hashimoto H, Okayasu N, Kameyama A, Onogi H, Nakagawasai O, Nakazawa T, Kurosawa T, Hao Y, Isaji T, Tadano T, Narimatsu H, Taniguchi N, Gu J (2011) Alpha1,6-fucosyltransferase-deficient mice exhibit multiple behavioral abnormalities associated with a schizophrenia-like phenotype: importance of the balance between the dopamine and serotonin systems. J Biol Chem., 286(21):18434–43. doi: 10.1074/jbc.M110.172536. [PubMed: 21471224]

Gaunitz S, Tjernberg LO, & Schedin-Weiss S (2021). The N-glycan profile in cortex and hippocampus is altered in Alzheimer disease. Journal of Neurochemistry, 159(2), 292–304. doi:10.1111/jnc.15202 [PubMed: 32986846]

Haenseler W, Sansom SN, Buchrieser J, Newey SE, Moore CS, Nicholls FJ, … Cowley SA (2017). A Highly Efficient Human Pluripotent Stem Cell Microglia Model Displays a Neuronal-Co-culture-Specific Expression Profile and Inflammatory Response. Stem Cell Reports, 8(6), 1727–1742. doi:10.1016/j.stemcr.2017.05.017 [PubMed: 28591653]

Heneka MT, Carson MJ, El Khoury J, Landreth GE, Brosseron F, Feinstein DL, … Kummer MP (2015). Neuroinflammation in Alzheimer's disease. Lancet Neurol, 14(4), 388–405. doi:10.1016/ S1474-4422(15)70016-5 [PubMed: 25792098]

Hong HS, Maezawa I, Budamagunta M, Rana S, Shi A, Vassar R, … Jin LW (2010). Candidate anti-A beta fluorene compounds selected from analogs of amyloid imaging agents. Neurobiol Aging, 31(10), 1690–1699. doi:10.1016/j.neurobiolaging.2008.09.019 [PubMed: 19022536]

Hooper C, Meimaridou E, Tavassoli M, Melino G, Lovestone S, & Killick R (2007). p53 is upregulated in Alzheimer's disease and induces tau phosphorylation in HEK293a cells. Neuroscience Letters, 418(1), 34–37. doi:10.1016/j.neulet.2007.03.026 [PubMed: 17399897]

Ihara H, Ikeda Y, Toma S, Wang X, Suzuki T, Gu J, … Taniguchi N (2007). Crystal structure of mammalian alpha1,6-fucosyltransferase, FUT8. Glycobiology, 17(5), 455–466. doi:10.1093/ glycob/cwl079 [PubMed: 17172260]

Jayadev S, Nesser NK, Hopkins S, Myers SJ, Case A, Lee RJ, … Garden GA (2011). Transcription factor p53 influences microglial activation phenotype. Glia, 59(10), 1402–1413. doi:10.1002/ glia.21178 [PubMed: 21598312]

Jin LW, Lucente JD, Nguyen HM, Singh V, Singh L, Chavez M, … Maezawa I (2019). Repurposing the KCa3.1 inhibitor senicapoc for Alzheimer's disease. Ann Clin Transl Neurol, 6(4), 723–738. doi:10.1002/acn3.754 [PubMed: 31019997]

Kapellos TS, Taylor L, Lee H, Cowley SA, James WS, Iqbal AJ, & Greaves DR (2016). A novel real time imaging platform to quantify macrophage phagocytosis. Biochem Pharmacol, 116, 107–119. doi:10.1016/j.bcp.2016.07.011 [PubMed: 27475716]

Kitamura Y, Shimohama S, Kamoshima W, Matsuoka Y, Nomura Y, & Taniguchi T (1997). Changes of p53 in the brains of patients with Alzheimer's disease. Biochemical and Biophysical Research Communications, 232(2), 418–421. doi:DOI 10.1006/bbrc.1997.6301 [PubMed: 9125193]

Kizuka Y, Nakano M, Yamaguchi Y, Nakajima K, Oka R, Sato K, … Taniguchi N (2017). An Alkynyl-Fucose Halts Hepatoma Cell Migration and Invasion by Inhibiting GDP-Fucose-Synthesizing Enzyme FX, TSTA3. Cell Chem Biol, 24(12), 1467–1478 e1465. doi:10.1016/ j.chembiol.2017.08.023 [PubMed: 29033318]

Kobayashi Y, Tateno H, Dohra H, Moriwaki K, Miyoshi E, Hirabayashi J, & Kawagishi H (2012). A novel core fucose-specific lectin from the mushroom Pholiota squarrosa. Journal of Biological Chemistry, 287(41), 33973–33982. doi:10.1074/jbc.M111.327692 [PubMed: 22872641]

Kotzler MP, Blank S, Bantleon FI, Spillner E, & Meyer B (2012). Donor substrate binding and enzymatic mechanism of human core alpha1,6-fucosyltransferase (FUT8). Biochim Biophys Acta, 1820(12), 1915–1925. doi:10.1016/j.bbagen.2012.08.018 [PubMed: 22982178]

Kumari R, & Jat P (2021). Mechanisms of Cellular Senescence: Cell Cycle Arrest and Senescence Associated Secretory Phenotype. Front Cell Dev Biol, 9, 645593. doi:10.3389/fcell.2021.645593 [PubMed: 33855023]

Lambert MP, Barlow AK, Chromy BA, Edwards C, Freed R, Liosatos M, … Klein WL (1998). Diffusible, nonfibrillar ligands derived from Abeta1-42 are potent central nervous system neurotoxins. Proc Natl Acad Sci U S A, 95(11), 6448–6453. doi:10.1073/pnas.95.11.6448 [PubMed: 9600986]

Lee J, Ha S, Kim M, Kim SW, Yun J, Ozcan S, … An HJ (2020). Spatial and temporal diversity of glycome expression in mammalian brain. Proc Natl Acad Sci U S A, 117(46), 28743–28753. doi:10.1073/pnas.2014207117 [PubMed: 33139572]

Leng F, & Edison P (2021). Neuroinflammation and microglial activation in Alzheimer disease: where do we go from here? Nat Rev Neurol, 17(3), 157–172. doi:10.1038/s41582-020-00435-y [PubMed: 33318676]

Li L, Zi X, Hou D, & Tu Q (2017). Kruppel-like factor 4 regulates amyloid-beta (Abeta)-induced neuroinflammation in Alzheimer's disease. Neurosci Lett, 643, 131–137. doi:10.1016/ j.neulet.2017.02.017 [PubMed: 28189744]

Lu X, Zhang D, Shoji H, Duan C, Zhang G, Isaji T, … Gu J (2019). Deficiency of alpha1,6-fucosyltransferase promotes neuroinflammation by increasing the sensitivity of glial cells to inflammatory mediators. Biochim Biophys Acta Gen Subj, 1863(3), 598–608. doi:10.1016/ j.bbagen.2018.12.008 [PubMed: 30572004]

Maezawa I, Nguyen HM, Di Lucente J, Jenkins DP, Singh V, Hilt S, … Jin LW (2017). Kv1.3 inhibition as a potential microglia-targeted therapy for Alzheimer's disease: preclinical proof of concept. Brain. doi:10.1093/brain/awx346

Maezawa I, Zimin PI, Wulff H, & Jin LW (2011). Amyloid-beta protein oligomer at low nanomolar concentrations activates microglia and induces microglial neurotoxicity. J Biol Chem, 286(5), 3693–3706. doi:M110.135244 [pii] 10.1074/jbc.M110.135244 [PubMed: 20971854]

Murrey HE, Gama CI, Kalovidouris SA, Luo WI, Driggers EM, Porton B, & Hsieh-Wilson LC (2006). Protein fucosylation regulates synapsin Ia/Ib expression and neuronal morphology in primary hippocampal neurons. Proc Natl Acad Sci U S A, 103(1), 21–26. doi:10.1073/pnas.0503381102 [PubMed: 16373512]

Ng BG, Rosenfeld JA, Emrick L, Jain M, Burrage LC, Lee B, … Freeze HH (2018). Pathogenic Variants in Fucokinase Cause a Congenital Disorder of Glycosylation. Am J Hum Genet, 103(6), 1030–1037. doi:10.1016/j.ajhg.2018.10.021 [PubMed: 30503518]

Nimmerjahn A, Kirchhoff F, & Helmchen F (2005). Resting microglial cells are highly dynamic surveillants of brain parenchyma in vivo. Science, 308(5726), 1314–1318. doi:1110647 [pii] 10.1126/science.1110647 [PubMed: 15831717]

Oakley H, Cole SL, Logan S, Maus E, Shao P, Craft J, … Vassar R (2006). Intraneuronal beta-amyloid aggregates, neurodegeneration, and neuron loss in transgenic mice with five familial Alzheimer's disease mutations: potential factors in amyloid plaque formation. J Neurosci, 26(40), 10129–10140. doi:10.1523/JNEUROSCI.1202-06.2006 [PubMed: 17021169]

Okagawa Y, Takada K, Arihara Y, Kikuchi S, Osuga T, Nakamura H, … Kato J (2016). Activated p53 with Histone Deacetylase Inhibitor Enhances L-Fucose-Mediated Drug Delivery through Induction of Fucosyltransferase 8 Expression in Hepatocellular Carcinoma Cells. PLoS One, 11(12), e0168355. doi:10.1371/journal.pone.0168355 [PubMed: 27977808]

Olausson J, Tibell L, Jonsson BH, & Pahlsson P (2008). Detection of a high affinity binding site in recombinant Aleuria aurantia lectin. Glycoconj J, 25(8), 753–762. doi:10.1007/s10719-008-9135-7 [PubMed: 18493851]

Penney J, Ralvenius WT, & Tsai LH (2019). Modeling Alzheimer's disease with iPSC-derived brain cells. Mol Psychiatry. doi:10.1038/s41380-019-0468-3

Puigdellivol M, Allendorf DH, & Brown GC (2020). Sialylation and Galectin-3 in Microglia-Mediated Neuroinflammation and Neurodegeneration. Front Cell Neurosci, 14, 162. doi:10.3389/fncel.2020.00162 [PubMed: 32581723]

Rillahan CD, Antonopoulos A, Lefort CT, Sonon R, Azadi P, Ley K, … Paulson JC (2012). Global metabolic inhibitors of sialyl- and fucosyltransferases remodel the glycome. Nat Chem Biol, 8(7), 661–668. doi:10.1038/nchembio.999 [PubMed: 22683610]

Romano PR, Mackay A, Vong M, DeSa J, Lamontagne A, Comunale MA, … Mehta A (2011). Development of recombinant Aleuria aurantia lectins with altered binding specificities to fucosylated glycans. Biochem Biophys Res Commun, 414(1), 84–89. doi:10.1016/j.bbrc.2011.09.027 [PubMed: 21945439]

Rustenhoven J, Park TI, Schweder P, Scotter J, Correia J, Smith AM, … Dragunow M (2016). Isolation of highly enriched primary human microglia for functional studies. Sci Rep, 6, 19371. doi:10.1038/srep19371 [PubMed: 26778406]

Saramaki A, Banwell CM, Campbell MJ, & Carlberg C (2006). Regulation of the human p21(waf1/cip1) gene promoter via multiple binding sites for p53 and the vitamin D3 receptor. Nucleic Acids Res, 34(2), 543–554. doi:10.1093/nar/gkj460 [PubMed: 16434701]

Schnaar RL, Gerardy-Schahn R, & Hildebrandt H (2014). Sialic acids in the brain: gangliosides and polysialic acid in nervous system development, stability, disease, and regeneration. Physiol Rev, 94(2), 461–518. doi:10.1152/physrev.00033.2013 [PubMed: 24692354]

Schneider M, Al-Shareffi E, & Haltiwanger RS (2017). Biological functions of fucose in mammals. Glycobiology, 27(7), 601–618. doi:10.1093/glycob/cwx034 [PubMed: 28430973]

Skurska E, Szulc B, Maszczak-Seneczko D, Wiktor M, Wiertelak W, Makowiecka A, & Olczak M (2022). Incorporation of fucose into glycans independent of the GDP-fucose transporter SLC35C1 preferentially utilizes salvaged over de novo GDP-fucose. Journal of Biological Chemistry, 298(8). doi:ARTN 102206 10.1016/j.jbc.2022.102206 [PubMed: 35772493]

Smith AM, & Dragunow M (2014). The human side of microglia. Trends Neurosci, 37(3), 125–135. doi:10.1016/j.tins.2013.12.001 [PubMed: 24388427]

Spittau B, Dokalis N, & Prinz M (2020). The Role of TGFbeta Signaling in Microglia Maturation and Activation. Trends in Immunology, 41(9), 836–848. doi:10.1016/j.it.2020.07.003 [PubMed: 32741652]

Stansley B, Post J, & Hensley K (2012). A comparative review of cell culture systems for the study of microglial biology in Alzheimer's disease. J Neuroinflammation, 9, 115. doi:10.1186/1742-2094-9-115 [PubMed: 22651808]

Sullivan KD, Galbraith MD, Andrysik Z, & Espinosa JM (2018). Mechanisms of transcriptional regulation by p53. Cell Death Differ, 25(1), 133–143. doi:10.1038/cdd.2017.174 [PubMed: 29125602]

Tan MS, Wang SY, Song JX, & Jia JP (2012). Combination of p53(ser15) and p21/p21(thr145) in peripheral blood lymphocytes as potential Alzheimer's disease biomarkers. Neuroscience Letters, 516(2), 226–231. doi:10.1016/j.neulet.2012.03.093 [PubMed: 22503900]

Tateno H, Nakamura-Tsuruta S, & Hirabayashi J (2009). Comparative analysis of core-fucose-binding lectins from Lens culinaris and Pisum sativum using frontal affinity chromatography. Glycobiology, 19(5), 527–536. doi:10.1093/glycob/cwp016 [PubMed: 19218400]

Tena J, & Lebrilla CB (2021). Glycomic profiling and the mammalian brain. Proc Natl Acad Sci U S A, 118(1). doi:10.1073/pnas.2022238118

Tu CF, Wu MY, Lin YC, Kannagi R, & Yang RB (2017). FUT8 promotes breast cancer cell invasiveness by remodeling TGF-beta receptor core fucosylation. Breast Cancer Res, 19(1), 111. doi:10.1186/s13058-017-0904-8 [PubMed: 28982386]

Wang M, Beckmann ND, Roussos P, Wang E, Zhou X, Wang Q, … Zhang B (2018). The Mount Sinai cohort of large-scale genomic, transcriptomic and proteomic data in Alzheimer's disease. Sci Data, 5, 180185. doi:10.1038/sdata.2018.185 [PubMed: 30204156]

Wang X, Gu J, Ihara H, Miyoshi E, Honke K, & Taniguchi N (2006). Core fucosylation regulates epidermal growth factor receptor-mediated intracellular signaling. Journal of Biological Chemistry, 281(5), 2572–2577. doi:10.1074/jbc.M510893200 [PubMed: 16316986]

Wang X, Inoue S, Gu J, Miyoshi E, Noda K, Li W, … Taniguchi N (2005). Dysregulation of TGF-beta1 receptor activation leads to abnormal lung development and emphysema-like phenotype in core fucose-deficient mice. Proc Natl Acad Sci U S A, 102(44), 15791–15796. doi:10.1073/pnas.0507375102 [PubMed: 16236725]

Wang X, Gu J, Miyoshi E, Honke K, Taniguchi N (2006) Phenotype changes of Fut8 knockout mouse: core fucosylation is crucial for the function of growth factor receptor(s). Methods Enzymol. 417, 11–22. doi: 10.1016/S0076-6879(06)17002-0. [PubMed: 17132494]

Yang Q, & Wang LX (2016). Mammalian alpha-1,6-Fucosyltransferase (FUT8) Is the Sole Enzyme Responsible for the N-Acetylglucosaminyltransferase I-independent Core Fucosylation of High-mannose N-Glycans. Journal of Biological Chemistry, 291(21), 11064–11071. doi:10.1074/jbc.M116.720789 [PubMed: 27008861]

Zhao Y, Itoh S, Wang X, Isaji T, Miyoshi E, Kariya Y, … Gu J (2006). Deletion of core fucosylation on alpha3beta1 integrin down-regulates its functions. Journal of Biological Chemistry, 281(50), 38343–38350. doi:10.1074/jbc.M608764200 [PubMed: 17043354]

Zhou QW, Xie YX, Lam M, & Lebrilla CB (2021). N-Glycomic Analysis of the Cell Shows Specific Effects of Glycosyl Transferase Inhibitors. Cells, 10(9). doi:ARTN 2318 10.3390/cells10092318 [PubMed: 34571967]

Main points

Amyloid-β oligomer-induced activation of human microglia, a pathogenic process in Alzheimer's disease, requires FUT8-catalyzed α1-6 core fucosylation of N-glycans. FUT8 is a component of the p53 signaling cascade regulating microglial behavior.
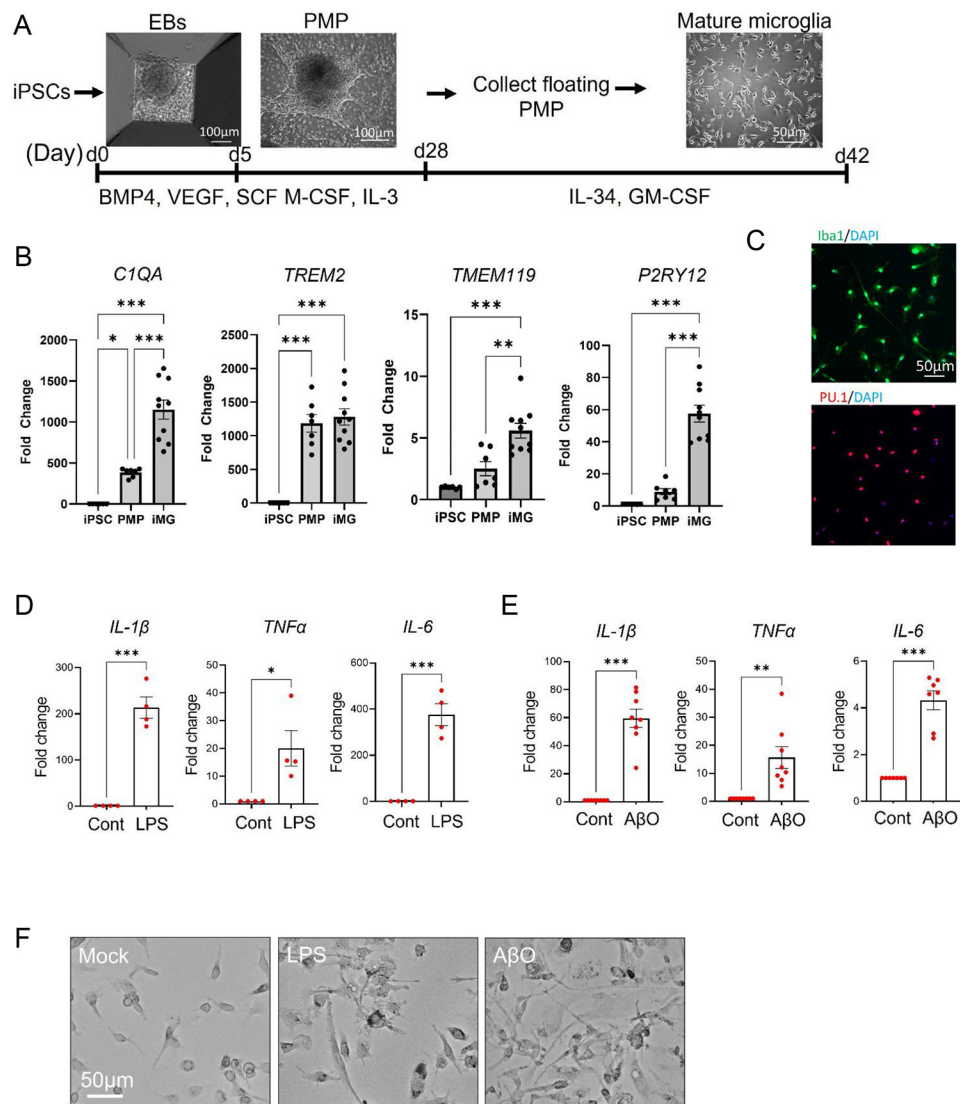
Figure 1.
Validation of hiMG. (**A**) Diagram depicting the major steps and time course of the microglial differentiation protocol. (**B**) Differentiated microglia show enhanced expression of mature microglia markers. Shown are qPCR data with the values of the iPSC group set as 1. $N = 7\text{-}10$; *$p<0.05$, **$p<0.01$, ***$p<0.001$; one-way ANOVA with Tukey's *post hoc* test. (**C**) Representative immunofluorescence micrographs of differentiated microglia stained with Iba1 (green) and PU.1 (red), and counterstained with DAPI (blue). (**D**) Differentiated microglia respond to LPS (100 ng/ml, $n = 4$, 24 hrs) and AβO (3 μM, $n = 7\text{-}8$, 24 hrs) with increased pro-inflammatory cytokine expressions. The increase is expressed in fold change normalized to the control group, the value of which is set as 1. *$p<0.05$, **$p<0.01$, ***$p<0.001$; Student's t-test. (**E**) The activation morphological changes following LPS and AβO stimulation of hiMG. All error bars indicate s.e.m.. For qPCR values comparisons, increases are expressed in fold changes normalized to the control groups with values set as 1.
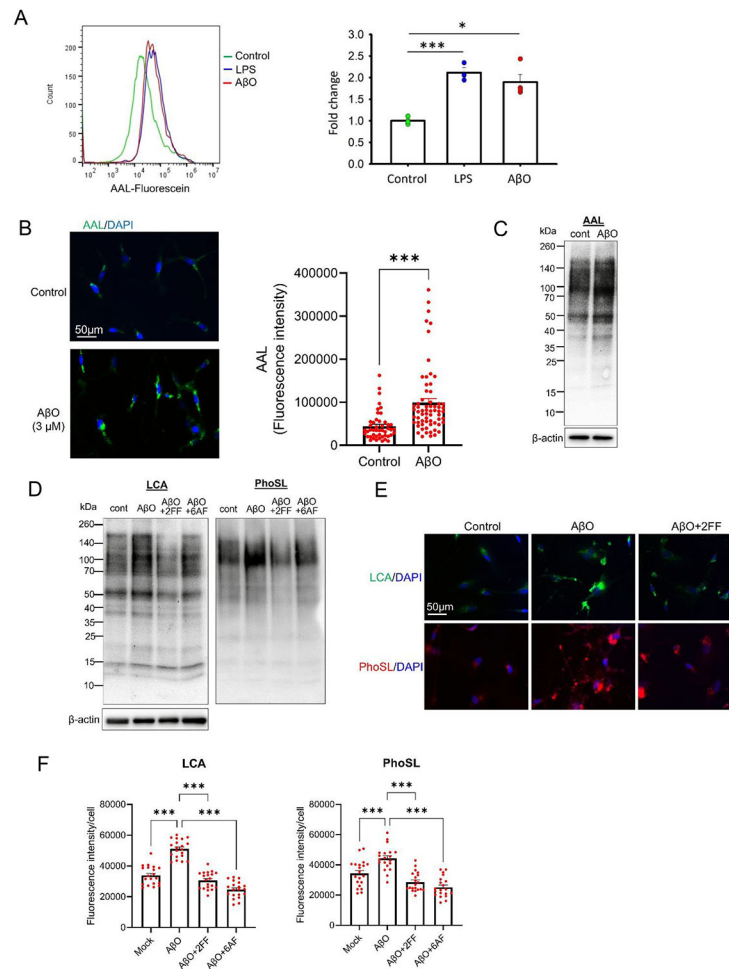
Figure 2.
AβO-activated hiMG show enhanced fucosylation, particularly core fucosylation. (**A**) Flow cytometry shows enhanced AAL-Fluorescein binding following LPS (100 ng/ml) and AβO (3 μM) stimulation for 24 hrs. Shown are representative traces and a bar graph summarizing fluorescence intensities from three independent experiments. Increases are expressed in fold changes normalized to the control group with the mean value set as 1. (**B**) Representative fluorescence images of AAL staining and a bar graph summarizing the fluorescence intensities of cells in 8 randomly selected fields per group from 6 independent experiments. ***p<0.001; Student's t-test. (**C**) Representative lectin blot with AAL. (**D-F**) AβO treatment enhances the binding of core fucosylation-specific lectins LCA and PhoSL, which is reduced by fucosylation inhibitors 2FF and 6AF. Representative lectin blots are shown in D and fluorescence images in E. F shows bar graphs summarizing fluorescence intensities of cells from 5 randomly selected fields in three independent experiments, ***p<0.001, one-way ANOVA with Tukey's *post hoc* test. All error bars indicate s.e.m..
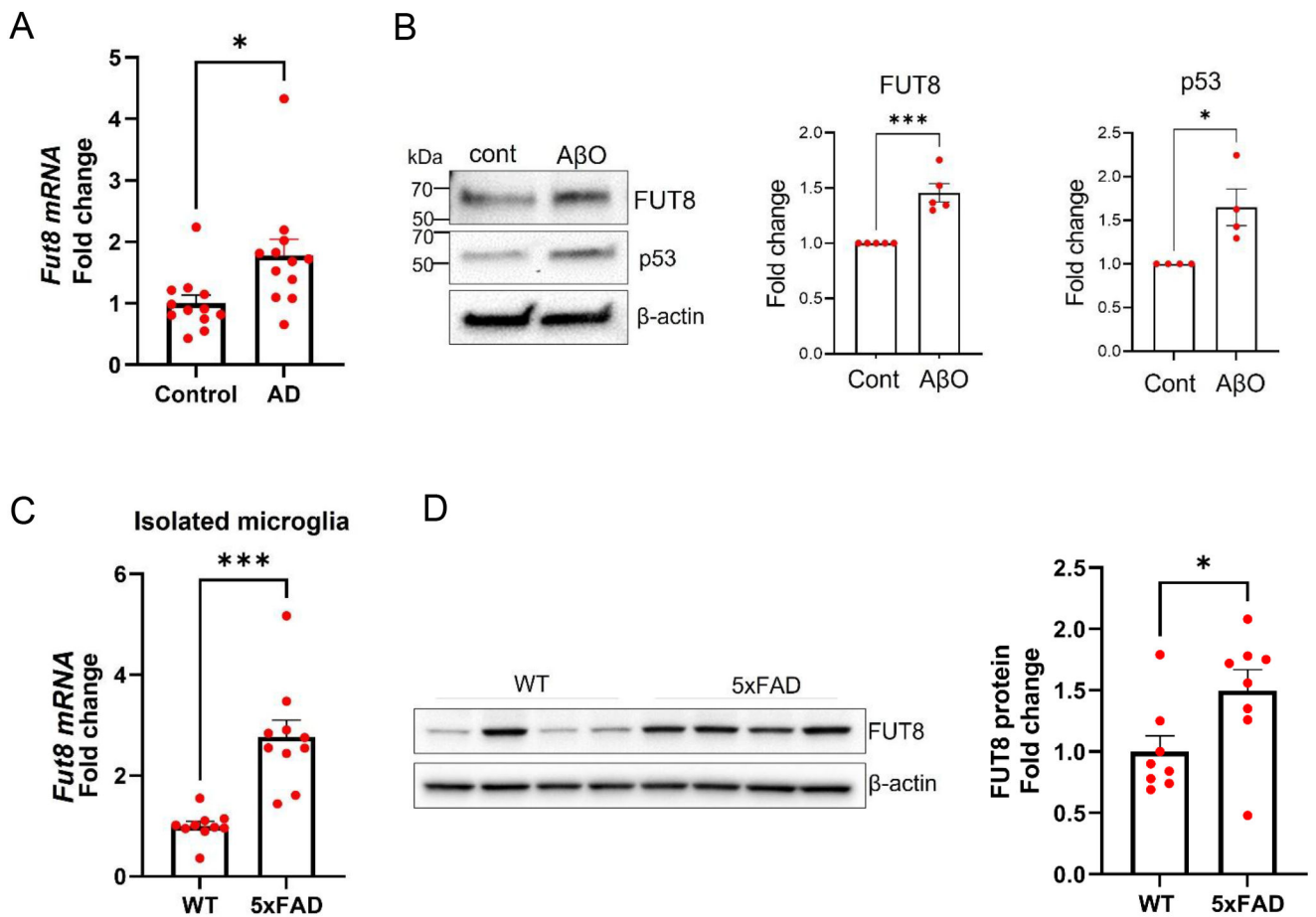
Figure 3.
FUT8 expression in AD samples and models. (**A**) Quantitative PCR shows that the transcript level of *Fut8* is increased (*$p<0.05$, Student's t-test) in the middle temporal cortex of human AD brains ($n = 12$) compared to age-matched, cognitively normal controls ($n = 12$). (**B**) AβO-activated hiMG show increased protein level of FUT8 and p53. Shown are representative Western blots and bar graphs summarizing band intensities from 5 (for FUT8) and 4 (for p53) independent experiments. *$p<0.05$, ***$p<0.001$; Student's t-test. (**C**) Quantitative PCR shows that the transcript level of *Fut8* is increased in microglia isolated from 12-months-old 5xFAD mice compared to those from age-matched wild-type mice. $N = 10$ mice per group, ***$p<0.001$; Student's t-test. (**D**) Western blotting shows increased FUT8 protein level in 5xFAD mice. Shown are a representative blot and a bar graph summarizing band intensities. $N = 8$ mice per group, *$p<0.05$; Student's t-test. All error bars indicate s.e.m.. For quantitative comparisons, value changes are expressed as fold changes normalized to the control groups with values set as 1.
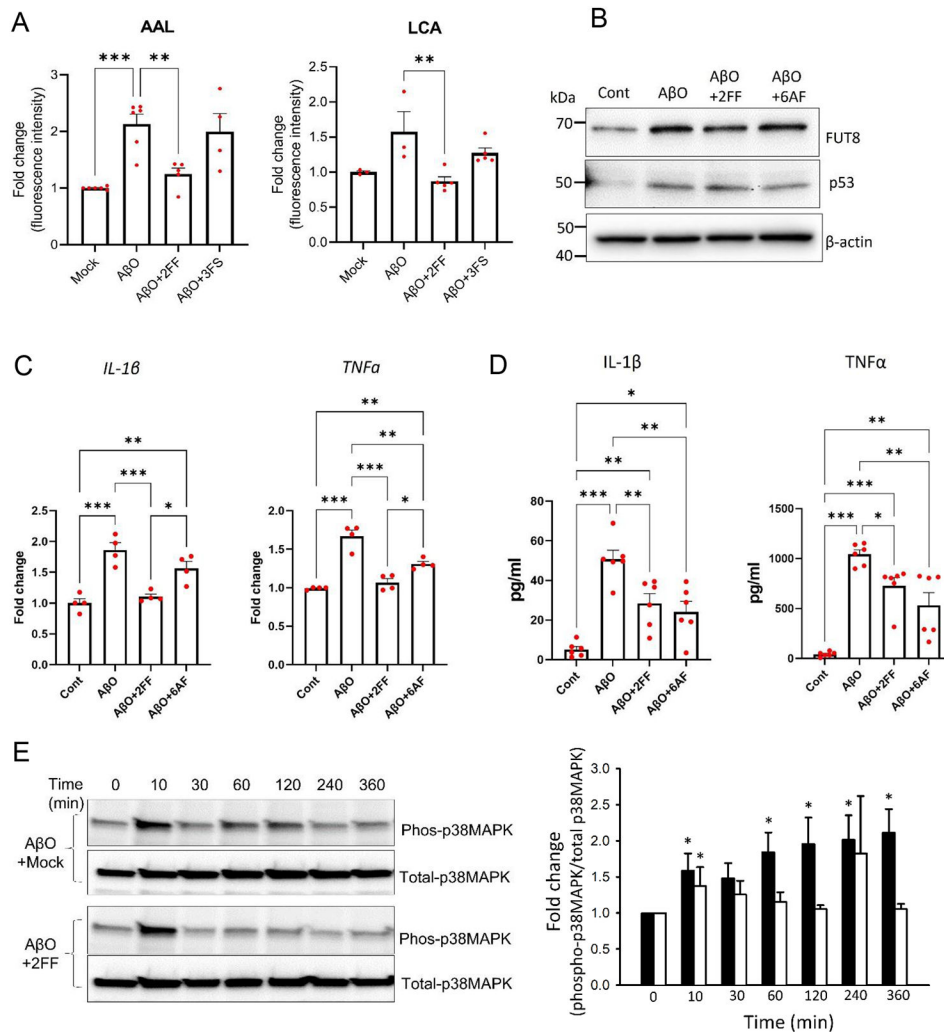
Figure 4.

Inhibition of fucosylation dampens AβO-induced hiMG activation. (**A**) Flow cytometry shows that the fucosylation inhibitor 2FF, but not the sialylation inhibitor 3FS, reduces AAL and LCA binding. AAL: n=4-6, LCA: n=3-5; $**p<0.01$, $***p<0.001$; one-way ANOVA with Tukey's *post hoc* test. (**B**) Western blotting shows that inhibition of fucosylation by 2FF and 6AF does not affect FUT8 and p53 protein expression. (**C-D**) Fucosylation inhibitors reduce AβO-induced pro-inflammatory cytokine production, shown by qPCR (C, $n = 4$) and ELISA (D, $n = 6$); $*p<0.05$, $**p<0.01$, $***p<0.001$; one-way ANOVA with Tukey's *post hoc* test. (**E**) Western blotting shows that phosphorylation of p38MAPK induced by AβO treatment is not sustained beyond 10-30 minutes post-treatment when fucosylation is inhibited by 2FF. The right panel shows quantification results from three independent experiments. The band intensity of phospho-p38MAPK induced by AβO treatment at the time post-treatment was normalized by that of total p38MAPK and the value was presented as fold changes relative to the value at 0 min, with or without 2FF. $*p<0.05$; Student's t-test compared to 0 min at each time point. All error bars indicate s.e.m.. For all quantitative comparisons, value changes are expressed as fold changes normalized to the control groups with values set as 1.
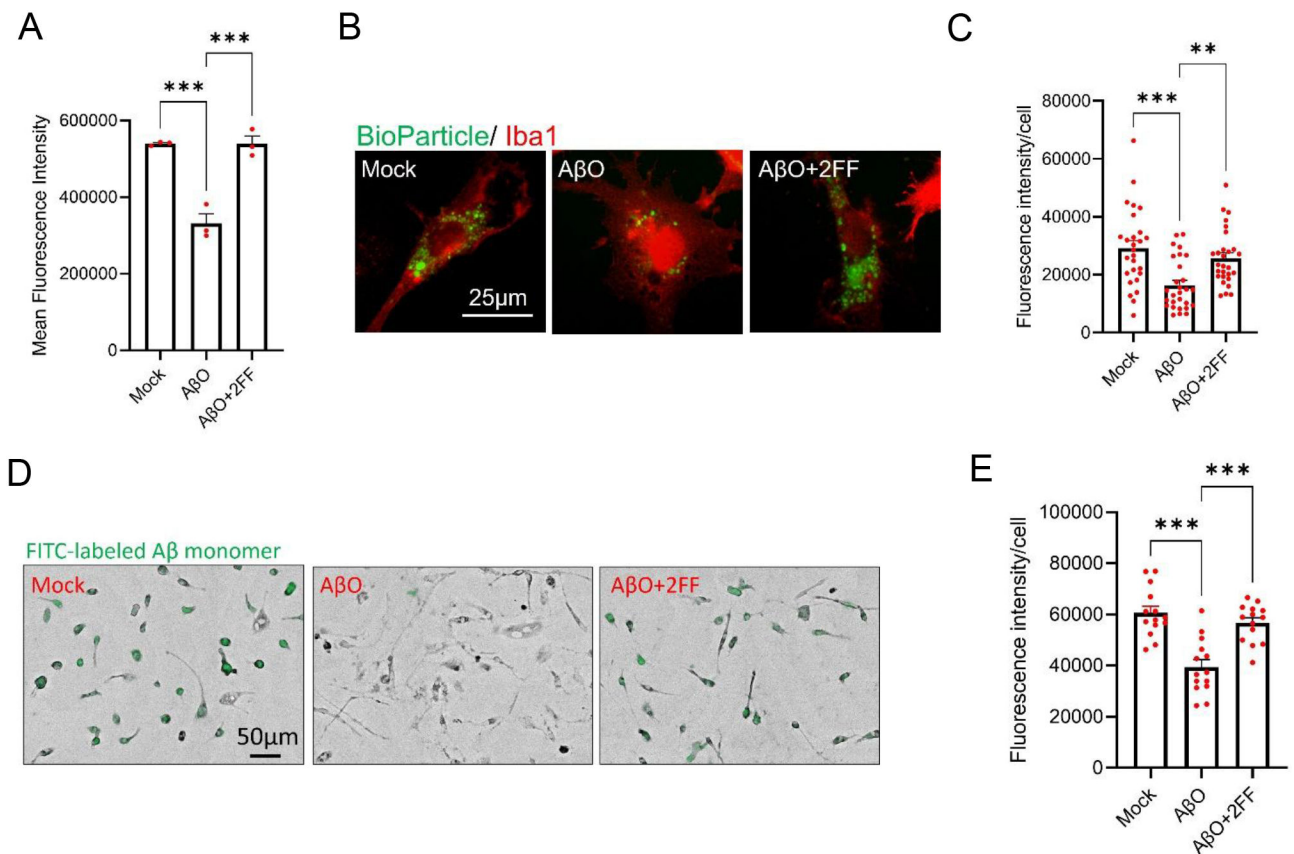
Figure 5.
AβO impairs hiMG phagocytotic capacity, which is rescued by inhibition of fucosylation. (**A**) Phagocytosis of pHrodo Green BioParticles analyzed by flow cytometry. $N =$ 3; ***$p<0.001$; one-way ANOVA with Tukey's *post hoc* test. (**B-C**) Phagocytosis of BioParticles visualized by fluorescence microscopy. Green: BioParticles; red: Iba1. Shown are representative fluorescence images (B) and a bar graph (C) summarizing the fluorescence intensities of cells in 9 randomly selected fields from three independent experiments; **$p<0.01$, ***$p<0.001$; one-way ANOVA with Tukey's *post hoc* test. (**D-E**) Phagocytosis of FITC-labeled Aβ peptide. Shown are representative combined fluorescence/ brightfield images (D) and a bar graph (E) summarizing the fluorescence intensities of cells in 6 randomly selected fields from three independent experiments; ***$p<0.001$; one-way ANOVA with Tukey's *post hoc* test. All error bars indicate s.e.m..
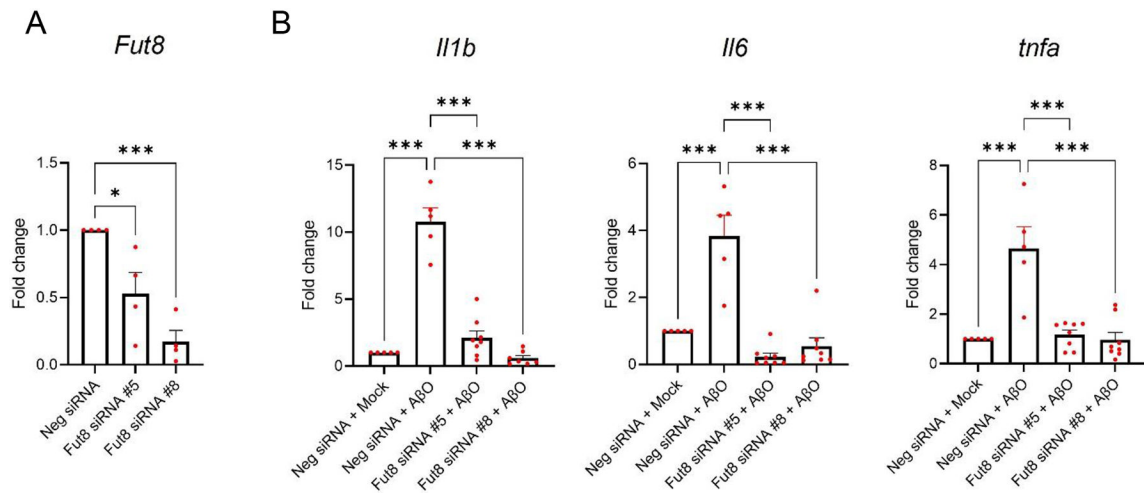
Figure 6.
Fut8 knockdown diminishes AβO-induced increases in pro-inflammatory cytokines. (**A**) The degrees of knockdown by two siRNAs shown by qPCR in four independent tests; $*p{<}0.05$, $***p{<}0.001$; one-way ANOVA with Tukey's *post hoc* test. (B) *Il1b*, *Il6*, and *tnfa* transcripts quantified by qPCR following *Fut8* knockdown. $N = 5\text{-}8$, $***p{<}0.001$; one-way ANOVA with Tukey's *post hoc* test. All error bars indicate s.e.m.. For quantitative comparisons, value changes are expressed as fold changes normalized to the control groups with values set as 1.
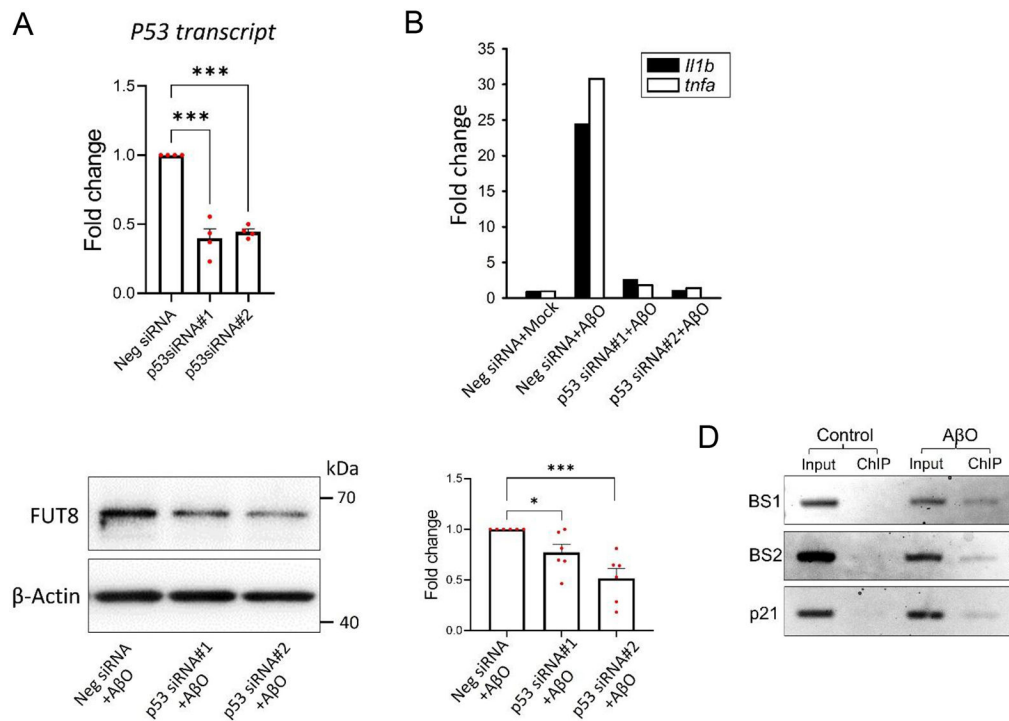
Figure 7.

P53 drives FUT expression in AβO-activated hiMG. (**A**) The degrees of *p53* knockdown by two siRNAs shown by qPCR in four independent tests; (**B**) *Il1b* and *tnfa* transcripts quantified by qPCR following *p53* knockdown. (**C**) Representative Western blot showing FUT8 down-regulation following *p53* knockdown, and a bar graph summarizing band intensities of FUT8 from 6 independent experiments. (**D**) ChIP assay shows that p53 binds to the two conserved binding sites (BS1 and BS2) in *Fut8* gene promoter following AβO treatment, with binding to a p21 promoter sequence as a positive control. *$p<0.05$ and ***$p<0.001$; one-way ANOVA with Tukey's *post hoc* test. All error bars indicate s.e.m.. For quantitative comparisons, value changes are expressed as fold changes normalized to the control groups with values set as 1.

Table 1.

Primers and primer sequences used for qPCR and ChIP assays

Gene (Invitrogen)	Primer Sequence
IL-1β (Human)	FW: GTGCAGTTCAGTGATCGTACAGG RV: CCACAGACCTTCCAGGAGAATG
IL-6 (Human)	FW: CCAGCTATGAACTCCTTCTC RV: GCTTGTTCCTCACATCTCTC
TNF-α (Human)	FW: CTCTTCTGCCTGCTGCACTTTG RV: ATGGGCTACAGGCTTGTCACTC
C1QA (Human)	FW: GTGACACATGCTCTAAGAAG RV: GACTCTTAAGCACTGGATTG
P2RY12 (Human)	FW: AAGAGCACTCAAGACTTTAC RV: GGGTTTGAATGTATCCAGTAAG
TREM2 (Human)	FW: TCTGAGAGCTTCGAGGATGC RV: GGGGATTTCTCCTTCAAGA
TMEM119 (Human)	FW: AGTCCTGTACGCCAAGGAAC RV: GCAGCAACAGAAGGATGAGG
BS1 (Human)	FW: ACCTGGCAAGAGAACGACTG RV: TTTAGCTGCCATCCCAAAAC
BS2 (Human)	FW: TATCCACCCCACCTCTGACT RV: GCTCAGTTTGGGTGTCATCA
β-Actin (Human)	FW: TCAAGATCATTGCTCCTCCTGAG RV: ACATCTGCTGGAAGGTGGACA
β-Actin (Mouse)	FW: TGTCCACCTTCCAGCAGATGT RV: AGCTCAGTAACAGTCCGCCTAGA
Gene (Bio-Rad)	**Primer**
FUT8 (Human)	qHsaCID0008117
FUT8 (Mouse)	qMmuCID0039633
p53 (Human)	qHsaCID0013658